

## SENSITIVITY TO CAVITATION AND TURBULENCE MODELS PARAMETERS IN ASYMMETRIC NOZZLES FLOW NUMERICAL SIMULATIONS

**Santiago Márquez Damián<sup>a,b</sup>, Tomás Leschiutta<sup>a,b</sup> and Miguel G. Coussirat<sup>c</sup>**

<sup>a</sup>*Centro de Investigación de Métodos Computacionales (CIMEC-CONICET/UNL), Predio Dr. Alberto Cassano, Colectora Ruta Nac. N° 168, Km. 0, Paraje El Pozo, Santa Fe, Argentina, <https://santafe.conicet.gov.ar/cimec/>*

<sup>b</sup>*Universidad Tecnológica Nacional, FRSF, Lavaise 610, Santa Fe, Argentina, [miguel.coussirat@frm.utn.edu.ar](mailto:miguel.coussirat@frm.utn.edu.ar) <http://www.frsf.utn.edu.ar/>*

<sup>c</sup>*Laboratorio de Modelado Aeroelasticidad (LaMA). Universidad Tecnológica Nacional, FRM, Rodríguez 273, Mendoza, Argentina, <https://www4.frm.utn.edu.ar/>*

**Keywords:** cavitation, turbulence, eddy viscosity models, fuel injector nozzles, computational fluid dynamics

**Abstract.** Cavitating flows are a complex phenomenon involving turbulent flow and phase change, both of which must be considered in its modeling. This study examines the sensitivity of the simulated flow in asymmetric nozzles to the cavitation and turbulence models calibration parameters involved. Building upon previous studies and using the Computational Fluid Dynamics tool OpenFOAM®, a more detailed investigation was performed based on the  $k - \omega$  SST turbulence model and the Schnerr-Sauer cavitation models for cases of quite developed cavitation. The results reinforce previous conclusions related to the suitable cavitation and turbulence models calibration on the representation of the cavitated zone.

## 1 INTRODUCTION

The cavitation phenomenon involves a complete evaporation/condensation cycle within a liquid phase flow interacting with confining walls. During evaporation, this local low-pressure level causes the initial single-phase flow to become a multiphase flow, i.e., a mixture of liquid and gas/vapour bubbles (Knapp et al., 1970; Brennen, 2014). Cavitation occurrence under turbulent flow conditions, always involves complex interactions between turbulence structures and multiphase dynamics. The viscous nature of the flow, particularly the interaction between free-stream turbulence and the boundary layer, is one of the main factors contributing to the scale effects on the inception of cavitation. High turbulence levels induce early laminar/turbulent transition, which, in turn can lead to the elimination of laminar separation, affecting cavitation inception (Singhal et al., 2002; Korkut and Atlar, 2002; Coussirat and Moll, 2021). Additionally, the presence of undissolved gas particles and turbulence can modify the bubbles surface stress and often mask any departure of this critical pressure  $p_c$  from the vapor pressure,  $p_v$ , becoming an added issue in the study of cavitation bubbles behaviour (Singhal et al., 2002; Brennen, 2005, 2014). Steady and unsteady cavitating flows occur in numerous engineering systems across various applications. Unsteady cavitation causes low-frequency pressure oscillations and high-frequency pressure pulses. These pressure oscillations are associated with the ‘mean’ cavity dynamics, while the pressure pulses are produced by cavity collapses. As a result, vibrations and acoustic noise are generated and propagated through the hydrodynamic and mechanical systems (Escaler et al., 2006). Due to the small geometrical scales in nozzles, it is generally not straightforward to distinguish between steady (incipient cavitation) and unsteady (quite/full developed cavitation) states, especially when determining the extent of unsteadiness in each case, see Fig. 1.

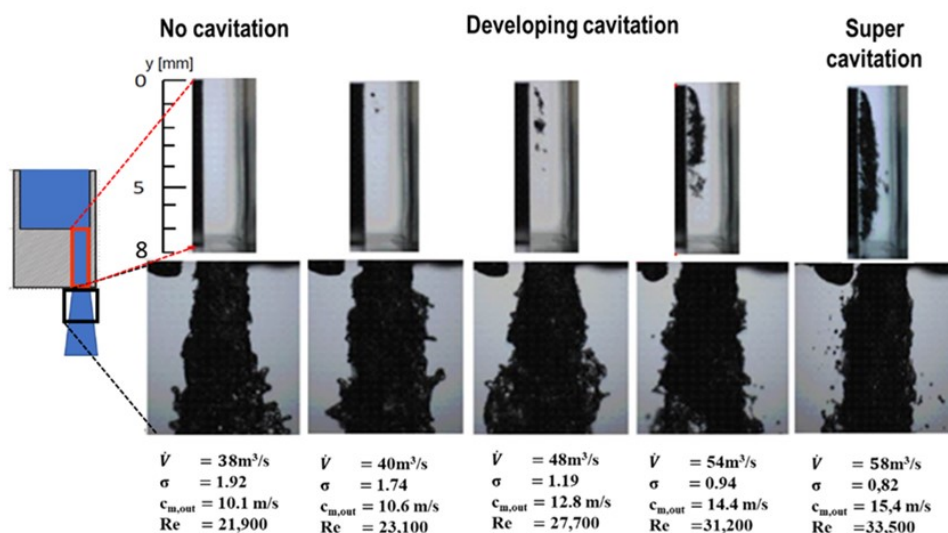


Figure 1: Cavitating flow experiment, showing cavity evolution and spray patterns for different inlet flow conditions (Sou et al., 2014). For detailed nomenclature and definitions see Section 2.

Cavitation occurrence in the nozzles is directly linked to the local pressure drop between its inlet and outlet, playing a significant role in the subsequent spray atomization at the outlet (Sou et al., 2014; Biçer and Sou, 2014; Biçer, 2015). Once developed cavitation occurs, it significantly influences the flow characteristics and spray breakup of the fuel. This type of cavitation

also induces erosion damage, compromising the injector's sealing. Both effects can severely impact injector performance. Despite its common occurrence, the frequency and mechanisms of the cloud shedding have yet to be thoroughly studied (He et al., 2023). A thorough understanding of the nozzle internal flow state is crucial for studying how cavitation affects diesel engine performance.

Owing to the high cost of conducting physical experiments on cavitation, which involve high-speed flow and small spatial and temporal scales, Computational Fluid Dynamics (CFD) has become a valuable tool for such studies. However, due to the complex nature of the flow, characterized by an abrupt phase change between a liquid and its vapor at nearly constant temperature and encompassing a multitude of complex flow phenomena, including multiphase flow, turbulence, instabilities, compressibility, and phase change, modeling such flows remains a challenging task (Wang et al., 2020). Several CFD codes have been specifically adapted or developed for modeling both turbulence and mass transfer in cavitating flows. For incompressible liquid-vapor-gas mixtures in CFD, a steady or unsteady Reynolds Averaged Simulation (RAS/URAS) model combined with an eddy-viscosity model and a phase fraction model is commonly used. Homogenous mixture models are employed to calculate the phase fraction due to their practicality and adaptability to large-scale cavitation cases. In these methods, the phases (liquid, vapor, and possibly gas) are treated using a scalar field,  $\alpha$ , representing the phase fraction. These methods can be divided into two main categories: (i) barotropic models (BM), where a state equation is adopted as a closing relation between the vapor/gas fraction and the pressure, e.g. Dellannoy and Kueny 1990; Reboud et al., 1998; Song and He, 1998; Qin et al., 2003; and Coutier-Delgosha et al., 2005 (see the complete aforementioned references in Savio et al. (2021)). (ii) Transport Equation Models (TEM), where the phase fraction is governed by a non-linear partial differential equation, whose form varies according to the model considered. The latter relies on two source/sink terms, which are needed to model the phenomena of vaporization and condensation. Several models have been developed to parametrize these processes as functions of resolved variables; among them, we mention: a) the Merkle et al. (1998) model in which the source terms are related to the density variation, proportional to the dynamic pressure; b) the Kunz et al. (2000) model, which uses the same vaporization source term as Merkle's model and a simplified Ginzburg-Landau potential for the condensation one; c) Senocak and Shyy, 2002, who used the mass-momentum conservation equation at the interface to evaluate the source terms as a function of known flow variables; d) Singhal et al. (2002), Zwart et al. (2004), and Schnerr and Sauer (2001), who based the source terms on the simplification of the Rayleigh-Plesset equation for the dynamic of a bubble; e) Saito et al. (2007), who evaluated the source terms based on the theory of evaporation and condensation on a plane surface. For all the already mentioned TEMs (also so-called Homogeneous mixture methods, HMM), excepted the Kunz and the Schnerr-Sauer models, see complete references in the work from (Savio et al., 2021). To be competitive at industrial application scale, these Computational Fluid Dynamics (CFD) simulation must achieve a satisfactory level of accuracy while also maintaining a low computational cost, which are directly related to the adopted turbulence simulation strategy.

A meticulous calibration of the Eddy Viscosity Models (EVM) and TEM enables the accurate capture of various cavitating flow characteristics due to the close correlation between the cavitation state and the turbulence level in the flow. This relationship is associated with the spatial distribution of the computed mixture eddy viscosity level, which is defined by a suitable turbulence scaling dependent on the EVM used. This fact is particularly crucial in cases where the HMM model explicitly depends on the turbulence state of the flow e.g., the Singhal et al. (2002) model. Due to the close relation between the cavitation inception/developing condition

and the turbulence level in the flow a ‘non-standard turbulence state’ appears, then a careful calibration of the turbulence model is necessary to improve these predictions. Overprediction of the turbulent viscosity leads to decrease the dynamic pressure yielding higher absolute pressure values and less cavitation. Then, the level of the vapour fraction and oscillation frequencies are commonly underpredicted by using uncalibrated EVM, (Coutier-Delgosha et al., 2003; Shi and Arafin, 2010; Biçer et al., 2013; Coussirat et al., 2016; Coussirat and Moll, 2021). On the other hand, an important issue related to the TEMs (Kunz and Schnerr-Sauer models) is the use of empirical coefficients, which are needed since the terms describing the condensation/vaporization processes are simplified version of complex physical relationship (the most indicative is perhaps the Schnerr-Sauer model, which considers only the terms of the Rayleigh-Plesset equation related to the asymptotic growth of bubbles). The condensation/vaporization coefficients  $C_c$  and  $C_v$  which, actually, act as accelerators/decelerators of the vaporization and condensation processes must be calibrated for the study of the specific problem (Villafranco et al., 2018; Savio et al., 2021).

This study is focused on the performance evaluation of calibrated TEMs implemented in the open-source code OpenFOAM® in cases of asymmetrical fuel nozzles where quite and developed cavitation is present. The goal is to facilitate future CFD applications to industrial problems involving this type of flow. Special attention was given to the cavity evolution prediction and the characteristic vortex shedding frequencies in all cases. This study emphasizes the TEMs performance under calibration. The EVM used was the SST model from Menter (1994), due to its proven effectiveness in previous works, despite that in these works was empathized that a calibration of this EVM is necessary too, see details in Coussirat et al. (2016); Coussirat and Moll (2021).

## 2 MODELLING METHODOLOGY

Cavitating flow in a Diesel injector, featuring an asymmetrical nozzle inlet configuration and a square section at the outlet (see Fig. 2), is investigated using Unsteady Reynolds Averaging Simulations (URAS) methodology. The SST  $k - \omega$  EVM (Cortes and Damián, 2023) coupled with the Schnerr and Sauer (2001) TEM, were used as numerical sub-models for the CFD simulations. Ad-hoc calibration strategies for the employed EVM and TEM were adopted, accounting for the fact that some reported CFD results obtained using steady/unsteady Reynolds Averaged Simulations (RAS/URAS) in cases of incipient/developing cavitation showed a higher dependence on the turbulence EVM rather than on the multiphase flow model used for computing the liquid fraction of the mixture (Sou et al., 2014; Biçer and Sou, 2014; Coussirat et al., 2016; Coussirat and Moll, 2021). Experimental data from Sou et al. (2014), were used to perform the calibration and validate the cavity characteristics.

Cavitation states at different flow regimes can be characterized by three dimensionless quantities, i.e., the Reynolds, Re; Strouhal, Sr and Cavitation numbers,  $\sigma$  as defined by Eq. (1)

$$\text{Re} = \frac{c_{m,out} w_n}{\nu} \quad \text{Sr} = \frac{f_{vs} L_{cav}}{c_{m,out}} \quad \sigma = \frac{p_{out} - p_v}{0.5 \rho c_{m,out}} \quad (1)$$

where  $p_{out}$  is the outlet pressure ( $1.0 \times 10^5$  Pa);  $p_v$  is the vapour pressure (2, 300 Pa);  $\rho$  is the liquid density ( $998 \frac{\text{kg}}{\text{m}^3}$ );  $c_{m,out}$  is the outlet mean flow velocity;  $w_n$  is the nozzle width;  $\nu$  is the liquid kinematic viscosity ( $1.0 \times 10^{-6} \frac{\text{m}^2}{\text{s}}$ );  $f_{vs}$  is the cavity shedding frequency; and  $L_{cav} = f(L_n)$  is the mean cavity length. This CFD study has tried to replicate the experiments of Sou et al., 2014. Comparisons were also made against the numerical results of Biçer (2015). Two distinct



2019). Consequently, these scales must be trackable in URAS simulations. RAS does not calculate individual eddy unsteady behavior, but URAS does. The mesh spacing should be sufficient to capture well integral scales and model/resolve the boundary layer. Insufficient mesh resolution leads to the dissipation of vortices due to numerical diffusion, making it challenging to onset the instability. Estimating the eddy lengths is necessary to ensure that the mesh has node spacing suitable for URAS/EVM simulations. This potential failure could occur independently of the mesh sensitivity study performed and could result in significant errors. Following the preceding discussion, already applied in previous works, a suitable two-dimensional (2D) structured mesh was defined for the nozzle computational domain. This mesh has  $5.0 \times 10^4$  hexahedral cells, ( $h = 0.04$  mm). To ensure both grid independence for the used 2D mesh and negligible differences in the predicted 2D and 3D flow fields from the numerical viewpoint, a grid sensitivity study was also conducted using the Grid Convergence Index (GCI) method, the Richardson extrapolation technique and a comparison with an extruded 3D geometry, i.e., approximately  $2.5 \times 10^6$  cells, see full details in (Coussirat et al., 2022). Extensive numerical tests have been performed by Schnerr and Sauer (2001) to identify the limit between the steady and unsteady cavitating flow regime. It was observed that the time dependent total vapor fraction, i.e., the integral value of the instantaneous local vapor fraction,  $\alpha$ , in the computational domain is dependent on the numerical time step, based on the single phase Courant–Friedrichs–Lewy condition, CFL. For  $CFL < 0.1$  the solutions include the resolution of secondary peaks which represents the instantaneous formation of a bubble cloud. For  $CFL > 0.1$  these details are no more resolved, and the corresponding oscillation frequency disappears. Then, the time production/dissipation scales were also estimated using these characteristic scales (Pope, 2000; Rodriguez, 2019), and compared with a time step calculated using the Courant–Friedrichs–Lewy (CFL) condition, see Eq. (2), where the cell length was used as a length scale to define a suitable time-step.

$$Co = \frac{\Delta t c_{m,out}}{h} \quad (2)$$

To capture a complete cycle of the energetic vortex shedding, a time step ten times minor than the particle residence time,  $t_{res}$  is desirable. Computing this time using the velocity into the nozzle and the nozzle length which is approximately  $10^{-5}$ s. However, the CFL condition imposes a smaller time-step for numerical stability. Then, the computed  $\Delta t$  for the simulations assuming  $Co = 0.15$  was of  $\Delta t = \mathcal{O}(1 \times 10^{-7}$  s), which satisfies both conditions. This combination of grid size and time step allows to simulate the behaviour of energetic eddies while avoid aliasing phenomena in the predicted vortex shedding. It's worth noting that a slightly larger time step could potentially be used while still adhering to both requirements. However, the chosen value ensures a conservative approach and minimizes potential numerical errors. This combination of space and time scales ensures an appropriate separation between the modelled and computed eddies, consistent with the capabilities of classical EVMs regarding the turbulent cascade modelling concept, (Pope, 2000; Rodriguez, 2019). It is important to emphasize that both mesh size sensitivity and turbulence scale analysis are crucial and should be performed together to guarantee mesh-independent results.

The open-source code OpenFOAM® was employed for all simulations. The Schnerr-Sauer cavitation model was used setting the coefficients as shown in Table 1, an additional laminar case was run using the setting of case F in order to check the influence of turbulence models given the low Reynolds number present in this case. After selecting the  $\sigma$  (see Fig. 1), the following boundary conditions were defined (see Fig. 2), for each case: Inlet (inflow): mean veloc-

| Case | $C_v$ |    |      | $C_c$ |     | $p_{sat}$         |                    |
|------|-------|----|------|-------|-----|-------------------|--------------------|
|      | 1     | 10 | 1000 | 0.01  | 0.1 | $2.3 \times 10^3$ | $10.3 \times 10^3$ |
| D    | ✓     |    |      | ✓     |     | ✓                 |                    |
| E    |       | ✓  |      | ✓     |     |                   | ✓                  |
| F    |       |    | ✓    |       | ✓   |                   | ✓                  |
| G    |       | ✓  |      |       | ✓   |                   | ✓                  |
| H*   |       |    | ✓    |       | ✓   | ✓                 |                    |

Table 1: Cases tested with  $k - \omega$  SST turbulence model,  $\beta^* = 0.09$ . H\* with  $\beta^* = 0.18$ . Schnerr-Sauer cavitation model in all cases.

ity in m/s, calculated from the flow rate; Outlet: pressure,  $p_{out} = 1.0 \times 10^5$  Pa (for all the cases); Walls: no-slip condition; Turbulence levels (inlet/outlet): Computed from the standard formulations for  $k$  and  $\omega$  (Rodríguez, 2019). The simulations used the `interPhaseChangeFoam` solver with the following discretization schemes: backward Euler in time, standard Gauss gradient, standard linear limited Gauss divergence term for momentum,  $k$  and  $\omega$ , vanLeer TVD advection for phase fraction with FCT limiter (Márquez Damián and Nigro, 2014). A saturation pressure value,  $p_{Sat}$ , higher than 2.300 Pa was defined due to the Singhal et al. (2002) recommendation to account for the influence of the turbulence over the cavitation model. Therefore, a correction of this saturation pressure based in Eq. (3) was computed

$$p_{Sat} = p_v + 0.195 \rho k \quad (3)$$

where the  $k$  value is obtained from an estimation of the kinetic energy and  $\rho$  is the mixture density.

## 4 RESULTS

Fig. 3 presents the results obtained by varying the the  $p_{Sat}$ ,  $C_v$  and  $C_c$  coefficients. The experiments from Sou et al. (2014) and the CFD results from Biçer (2015) were also included for comparison. The fine mesh used in Biçer (2015) is similar to the one used in the present CFD simulations. In the laminar case (without turbulence model) a locally refined mesh was used applying a binary subdivision to the inlet nozzle zone. The final mesh step is equivalent to a half of the used in Mesh 1 from Coussirat and Moll (2021). This mesh was defined to capture the main turbulence structures in the sense of a DNS simulation. The  $p_{Sat}$  was calculated using Eq. 3 (see Table 1), using a preliminary  $k$  value obtained from the inlet boundary condition, which was adjusted throughout the simulations. In the laminar case the  $p_{Sat}$  was also affected by the 'turbulence effect' correction, as in Eq. (3).

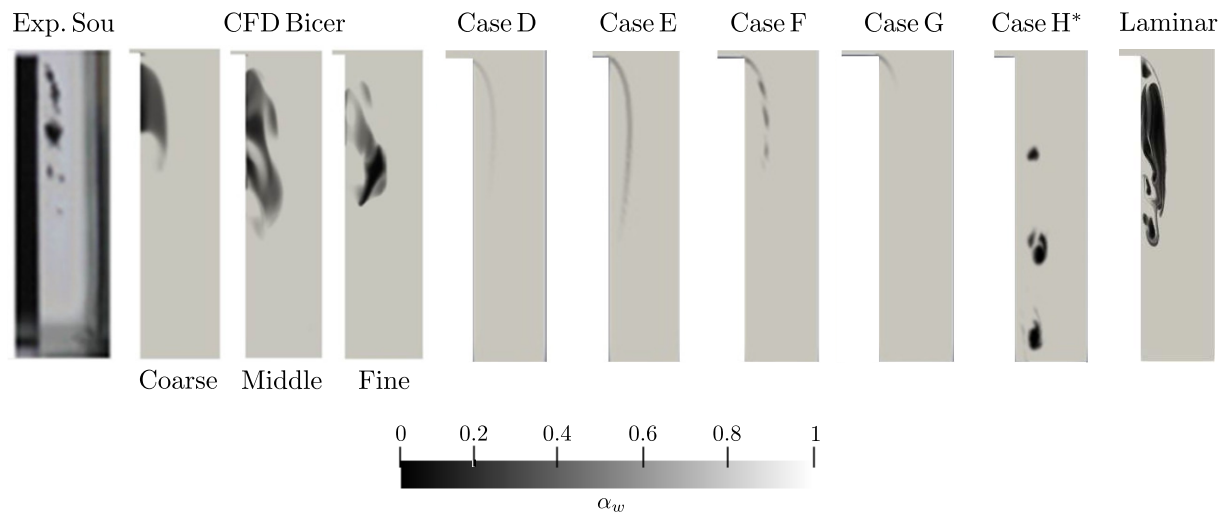


Figure 3: Water fraction for experimental and simulated cases

In cases D, E, F, G the cavity behavior is not accurately predicted both in the level of the vapor fraction,  $\alpha = 1 - \alpha_w$ , and in the cavity shape. Case F begins to exhibit a 'quasi-unsteady' cavity shape, as observed in the experiments, but with a significantly underpredicted  $\alpha$  level. For case H, the  $\beta^*$  parameter was also changed. This parameter is a key component of the turbulence model, influencing the  $\omega$  production and  $k$  dissipation terms in the SST  $k - \omega$  model. This, in turn, affects the turbulence level within the flow.  $\beta^*$  was calibrated empirically for this case, and we found that it had a more significant impact on the predicted  $\alpha$  levels than the  $C_v$  and  $C_c$  coefficients. A new case, not shown here, with a different  $p_{Sat}$ , i.e., 10,300 Pa, but with the same values for the  $C_v$  and  $C_c$  coefficients as in case H\*, predicts a higher  $\alpha$  level how was expected. This confirms that  $\beta^*$  has greater influence. Finally, the laminar case, as shown in Fig. (3), predicts a higher  $\alpha$  level than the other cases. This increase may be due to the lack of turbulence modelling, further supporting the trend observed when changing the  $\beta^*$  coefficient.

## 5 CONCLUSIONS

This study demonstrated that CFD is an effective tool for predicting cavitation dynamics in nozzles, capturing the behavior of cavitation clouds by describing the processes of generation, shedding, and collapse. The cavitation and turbulence models are strongly interconnected, but the relationship between the empirical tuning parameters in the cavitation model is unclear. Calibrating the turbulence model to adjust the predicted turbulence level follows trends seen in previous studies, suggesting that turbulence model calibration has a greater impact than cavitation model calibration. The present empirical parameters sensitivity analysis could help us understand the model's correlation. Furthermore, since both cavitation and turbulence affect the macroscopic flow pattern, they must be modeled simultaneously. The findings of this sensitivity study may motivate a more accurate calibration or development of these models, focusing on accounting for the interdependency of turbulence as thoroughly as possible.

## ACKNOWLEDGEMENTS

Financial support from the Universidad Tecnológica Nacional, Argentina (research projects AMTCAME0008441TC and ASTCFE0008685TC) is gratefully acknowledged.

## REFERENCES

- Biçer B. *Numerical simulation of cavitation phenomena inside fuel injector nozzles*. Ph.D. thesis, Kobe University, 2015.
- Biçer B. and Sou A. Numerical simulation of turbulent cavitating flow in diesel fuel injector. In *Proceedings of the 3rd International Symposium of Maritime Sciences, Kobe, Japan*, volume 3, pages 33–38. 2014.
- Biçer B., Tanaka A., Fukuda T., and Sou A. Numerical simulation of cavitation phenomena in diesel injector nozzles. In *Int. 16th Annual Conf. ILASS-ASIA*, pages 58–65. 2013.
- Brennen C. *Fundamentals of multiphase flow*. Cambridge University Press, 2005.
- Brennen C. *Cavitation and bubble dynamics*. Cambridge University Press, 2014.
- Cortes F. and Damián M. Evaluación de modelos turbulentos para la obtención del perfil energía cinética turbulenta. Flujo en placa plana. In *Mecánica Computacional Vol XXXIX*, pages 413–422. 2023.
- Coussirat M. and Moll F. Recalibration of eddy viscosity models for numerical simulation of cavitating flow patterns in low pressure nozzle injectors. *Journal of Fluids Engineering*, 143(3):031503, 2021.
- Coussirat M., Moll F., Cappa F., and Fontanals A. Study of available turbulence and cavitation models to reproduce flow patterns in confined flows. *Journal of Fluids Engineering*, 138(9):091304, 2016.
- Coussirat M., Moll F., and Leschiutta T. Scale adaptive simulations applied to fully cavitating turbulent flow in injector nozzles. *Mecánica Computacional*, 39(11):397–406, 2022.
- Coutier-Delgosha O., Reboud J., and Delannoy Y. Numerical simulation of the unsteady behaviour of cavitating flows. *International journal for numerical methods in fluids*, 42(5):527–548, 2003.
- Escaler X., Egusquiza E., Farhat M., Avellan F., and Coussirat M. Detection of cavitation in hydraulic turbines. *Mechanical systems and signal processing*, 20(4):983–1007, 2006.
- He J., An Q., Jin J., Feng S., and Zhang K. Experimental study and simulation of cavitation shedding in diesel engine nozzle using proper orthogonal decomposition and large eddy simulation. *Journal of Thermal Science*, 32(4):1487–1500, 2023.
- Knapp R., Daily J., and Hammit F. *Cavitation*. McGraw-Hill, 1970.
- Korkut E. and Atlar M. On the importance of the effect of turbulence in cavitation inception tests of marine propellers. *Proceedings of the Royal Society of London. Series A: Mathematical, Physical and Engineering Sciences*, 458(2017):29–48, 2002.
- Kunz R.F., Boger D.A., Stinebring D., Chyczewski T., Lindau J., Gibeling H., Venkateswaran S., and Govindan T. A preconditioned navier–stokes method for two-phase flows with application to cavitation prediction. *Computers & Fluids*, 29(8):849–875, 2000.
- Márquez Damián S. and Nigro N. An extended mixture model for the simultaneous treatment of small-scale and large-scale interfaces. *International Journal for Numerical Methods in Fluids*, 75(8):547–574, 2014.
- Menter F. Two-equation eddy-viscosity turbulence models for engineering applications. *AIAA journal*, 32(8):1598–1605, 1994.
- Merkle C., Feng J., and Buelow P. Computational modeling of the dynamics of sheet cavitation. In *Proceedings Third International Symposium on Cavitation*. Grenoble, France, 1998.
- Mitroglou N., Stamboliyski V., Karathanassis I., Nikas K., and Gavaises M. Cloud cavitation vortex shedding inside an injector nozzle. *Experimental Thermal and Fluid Science*, 84:179–189, 2017.

- Pope S. *Turbulent flows*. Cambridge University Press, 2000.
- Rodriguez S. *Applied Computational Fluid Dynamics and Turbulence Modeling: Practical Tools, Tips and Techniques*. Springer Nature, 2019.
- Saito Y., Takami R., Nakamori I., and Ikohagi T. Numerical analysis of unsteady behavior of cloud cavitation around a NACA0015 foil. *Computational Mechanics*, 40:85–96, 2007.
- Savio A., Cianferra M., and Armenio V. Analysis of performance of cavitation models with analytically calculated coefficients. *Energies*, 14(19):6425, 2021.
- Schnerr G. and Sauer J. Physical and numerical modeling of unsteady cavitation dynamics. In *Fourth international conference on multiphase flow*, volume 1, pages 1–12. ICMF New Orleans New Orleans, LO, USA, 2001.
- Shi J. and Arafin M. Cfd investigation of fuel property effect on cavitating flow in generic nozzle geometries. *ILASS-Europe 2010*, 2010.
- Singhal A., Athavale M., Li H., and Jiang Y. Mathematical basis and validation of the full cavitation model. *J. Fluids Eng.*, 124(3):617–624, 2002.
- Sou A., Biçer B., and Tomiyama A. Numerical simulation of incipient cavitation flow in a nozzle of fuel injector. *Computers & Fluids*, 103:42–48, 2014.
- Stanley C., Barber T., and Rosengarten G. Re-entrant jet mechanism for periodic cavitation shedding in a cylindrical orifice. *International Journal of Heat and Fluid Flow*, 50:169–176, 2014.
- Trummler T., Schmidt S., and Adams N. Investigation of condensation shocks and re-entrant jet dynamics in a cavitating nozzle flow by large-eddy simulation. *International Journal of Multiphase Flow*, 125:103215, 2020.
- Villafranco D., Do H., Grace S., Ryan E., and Holt R.G. Assessment of cavitation models in the prediction of cavitation in nozzle flow. In *Fluids Engineering Division Summer Meeting*, volume 51562, page V002T16A003. American Society of Mechanical Engineers, 2018.
- Wang C., Wang G., and Huang B. Characteristics and dynamics of compressible cavitating flows with special emphasis on compressibility effects. *International Journal of Multiphase Flow*, 130:103357, 2020.
- Wang Z., Zhang M., Kong D., Huang B., Wang G., and Wang C. The influence of ventilated cavitation on vortex shedding behind a bluff body. *Experimental Thermal and Fluid Science*, 98:181–194, 2018.
- Zwart P., Gerber A., and Belamri T. A two-phase flow model for predicting cavitation dynamics. In *In Fifth International Conference on Multiphase Flow*. Yokohama, Japan., 2004.